J. Biochem. 2010;148(3):289–298 doi:10.1093/jb/mvq068

JB THE JOURNAL OF BIOCHEMISTRY

In vitro evaluation of cellular responses induced by stable fullerene C_{60} medium dispersion

Received May 19, 2010; accepted June 11, 2010; published online June 23, 2010

Masanori Horie[1,*], Keiko Nishio[1], Haruhisa Kato[2], Naohide Shinohara[3], Ayako Nakamura[2], Katsuhide Fujita[3], Shinichi Kinugasa[2], Shigehisa Endoh[4], Kazuhiro Yamamoto[5], Osamu Yamamoto[6], Etsuo Niki[1], Yasukazu Yoshida[1] and Hitoshi Iwahashi[1]

[1]Health Research Institute (HRI), National Institute of Advanced Industrial Science and Technology (AIST), 1-8-31 Midorigaoka, Ikeda, Osaka 563-8577; [2]National Metrology Institute of Japan (NMIJ), AIST, 1-1-1 Higashi, Tsukuba, Ibaraki 305-8565; [3]Research Institute of Science for Safety and Sustainability (RISS), AIST, 16-1 Onogawa, Tsukuba, Ibaraki 305-8569; [4]Research Institute for Environmental Management Technology (EMTECH), AIST, Particle Measurement Group, 16-1 Onogawa, Tsukuba, Ibaraki 305-8569; [5]Research Institute of Instrumentation Frontier (RIIF), AIST, 1-1-1, Umezono, Tsukuba, Ibaraki 305-8565; and [6]Division of Dermatology, Tottori University Faculty of Medicine, Yonago, Tottori 683-8503, Japan

*Masanori Horie, Health Research Institute, National Institute of Advanced Industrial Science and Technology (AIST), 1-8-31 Midorigaoka, Ikeda, Osaka 563-8577, Japan. Tel: +81 72 751 9693, Fax: +81 72 751 9964, email: masa-horie@aist.go.jp

Because of the expansion of the functionalities available for modification of fullerene C_{60} and its derivatives, their uses are increasing. However, the consequences of fullerene exposure to human health have not been fully studied. *In vitro* experiments are useful for risk assessment and for understanding potential applications. However, the insolubility of pristine C_{60} in water makes the *in vitro* evaluation of cellular responses difficult. To overcome this problem, we prepared a stable and uniform C_{60}-medium dispersion for *in vitro* examinations. In addition, we examined the effect of the C_{60}-medium dispersion on human keratinocyte HaCaT cells and human lung carcinoma A549 cells to understand the cellular responses induced by exposure to C_{60}. Results indicated that exposure to C_{60} did not affect cell viability; neither apoptosis nor necrosis were induced, while cell proliferation was inhibited. Furthermore, intracellular oxidative stress was induced by C_{60} exposure in both HaCaT and A549 cells. Transmission electron microscopy indicated the cellular uptake of C_{60} aggregates. The results obtained from this study indicate that C_{60} has oxidative stress induction potential. Further examinations including *in vivo* studies are necessary for a more accurate evaluation of biological influences by C_{60}.

Keywords: Fullerene/culture cell/oxidative stress/stable dispersion/clonogenic assay.

Abbreviations: DMEM, Dulbecco's modified Eagle medium; FBS, foetal bovine serum; ROS, reactive oxygen species; DCFH-DA, 2′,7′-dichlorofluorescein diacetate.

Fullerene C_{60} is a molecule ~0.7 nm in diameter which consisting of 60 carbon atoms (*1*). Since its discovery in 1985 by Kroto *et al*., many different applications of C_{60} in industry, biology and medicine have been studied. A number of C_{60} derivatives are also reported (*2*), some of which showed antioxidant activity in cultured cells, such as the polyhydroxylated fullerene derivative $C_{60}(OH)_x$ or the cystine C_{60} derivative (*3–5*). In particular, cystine C_{60} protected rat pheochromocytoma PC12 cells from apoptotic cell death induced by hydrogen peroxide (*5*). Fullerene derivatives are utilized in cosmetics because of their antioxidant activities and their apparent safety. However, toxicity evaluation of pristine C_{60}, the chemical precursor of the derivatives, has been controversial. Some evidence suggests that C_{60} can induce oxidative stress. As an example, C_{60} stimulated by visible light generated singlet oxygen, caused lipid peroxidation and subsequently, 8-hydroxydeoxyguanosine (8-OH-dG) formation (*6*). It has also been reported that pristine C_{60} induced lipid peroxidation of cell membranes (*7*), intratracheal instillation of C_{60} to rat lung induced lipid peroxidation (*8*), and that treatment of cultured cells with C_{60} led to an increase in necrotic cells death but treatment with C_{60}(OH)n did not (*9*). Compared with C_{60}(OH)24, a highly water-soluble C_{60} derivative, C_{60} appears to be more cytotoxic (*10*). There are also reports that C_{60} behaves as an antioxidant. Polyvinylpyrrolidone (PVP)-entrapped C_{60}, which is soluble in water, showed antioxidant activity against reactive oxygen species (ROS) (*11*), indicating that pristine C_{60} has higher cytotoxic potential than water-soluble C_{60} derivatives. There is also a report suggesting that C_{60} may induce inflammatory responses as intratracheal instillation of fullerene C_{60} to mice resulted in an increase of cytokine levels (*12*).

Comprehensive evaluation and clarification of toxic mechanisms by *in vivo* examinations are also required for risk assessments. *In vitro* examinations demand dispersal of C_{60} into aqueous culture medium, but C_{60} is hardly soluble in water. This characteristic is one of the major causes of data incoherence of cellular responses to C_{60}. Culture medium for mammalian cells generally includes amino acids, salts and vitamins. In many cases, foetal bovine serum is added to the medium for healthy cell growth and then, proteins and lipids are included in the medium. As a result, cell culture

medium contains many electrolytes. Such electrolyte-rich solutions promote the formation of aggregates and agglomeration of C_{60} (*13*, *14*), and C_{60} aggregates have the potential to behave as nanoparticles. The large aggregates will accumulate onto cells via gravity sedimentation and the small aggregates will enter the cells by diffusion. A concentration gradient of aggregates is formed in the medium and the concentration of dispersion does not correlate with 'cellular exposure concentrations' (*15*, *16*). Therefore, determination of dispersion stability is important for *in vitro* examination of nanoparticles. Previous studies of cellular influences by C_{60} used dispersants such as tetrahydrofuran (THF) or Tween 80 to obtain a stable C_{60}-aqueous dispersion (*17–20*). Alternatively, the C_{60} was covered with PVP without modifying the C_{60} itself (*11*). Although these dispersion techniques are excellent for industrial purposes, it is unclear whether the technique is suitable for *in vitro* toxicity assessment. For example, Tween 80 increases the susceptibility of rat thymocytes to oxidative stress (*21*). Recently, the dispersion of C_{60} into aqueous solution using serum albumin has also been reported (*22*, *23*). However, there has been no investigation of the cellular responses induced by pristine C_{60} aggregates using stable dispersion methods. Here we have chosen to focus on the cellular responses of oxidative stress.

Materials and Methods

Cell culture

Human keratinocyte HaCaT cells were purchased from the German Cancer Research Center (DKFZ, Heidelberg, Germany). Human lung carcinoma A549 cells were purchased from the RIKEN BioResource Center (Tsukuba, Ibaraki, Japan). These cells were cultured in Dulbecco's modified Eagle medium (DMEM; Gibco, Invitrogen Corporation, Gland Island, NY) supplemented with 10% heat-inactivated foetal bovine serum (FBS; CELLect GOLD; MP Biomedicals Inc., Solon, OH), 100 units/ml of penicillin, 100 μg/ml of streptomycin and 250 ng/ml of amphotericin B (Nacalai Tesque Inc., Kyoto, Japan). Hereinafter this DMEM cocktail is called 'DMEM–FBS'. The DMEM cultures were placed in a 75-cm^2 flask (Corning Incorporated, Corning, NY) and incubated at 37°C in a 5% CO_2 atmosphere. For cell viability assays, cells were seeded in 96- or 6-well plates (Corning Inc.) at 2×10^5 cells/ml and incubated for 24 h; subsequently, the culture medium was removed, exposed to the C_{60} dispersion and incubated for another 6 or 24 h.

Preparation of C_{60} medium dispersion

C_{60} fullerene (market name nanom purple SU), was obtained from the Frontier Carbon Corporation (Kitakyushu, Fukuoka, Japan). High-concentration and low-concentration C_{60} dispersions were prepared as follows. C_{60} powder was dispersed in FBS solution at 10 mg/ml and stirred for 2 h. Next, 60 ml of this dispersion was added to 250 ml of DMEM–FBS and the mixture was pulverized for 30 min with 50 μm-zirconia beads using a bead mill at an agitation rate of 15.0 m/s under a nitrogen purge. Then, 300 ml of DMEM was added to the mixture in the bead mill and pulverized for a further 1 h. A total of 300 ml of this mixture was used as the high-concentration C_{60} dispersion, represented as No. 2 in Table I. Next, 60 ml of freshly prepared C_{60}–FBS dispersion and 250 ml of DMEM were added to the C_{60}–DMEM–FBS dispersion remaining in the bead mill, and the solution was stirred for 60 min. A volume of 500 ml of this C_{60}–DMEM–FBS dispersion was collected as the high-concentration C_{60} dispersion, designated as No.1 in Table I. Both these dispersions were centrifuged at 1000*g* for 10 min, 2000*g* for 10 min, 4000*g* for 10 min and 8000*g* for 45 min. The supernatant was collected and used as the C_{60} dispersion. The dispersions were passed through a filter of pore size 0.45 μm (Corning Incorporated) to sterilize the dispersion. Low-concentration C_{60} dispersions were obtained by preparing 5-fold and 10-fold dilutions of the high-concentration C_{60} dispersion No.2 with DMEM–FBS.

Characterization of C_{60} medium dispersion

Secondary particles are defined as a complex of aggregates of primary particles formed by the adsorption of some medium components and proteins contained in FBS. The average particle size is defined as the size of the secondary particles estimated by measuring the intensity of the light scattered by the particles, assuming that the aggregate is globular. The C_{60}–DMEM–FBS dispersion prepared by the aforementioned method was divided into three parts that were used simultaneously for biological examinations, C_{60}-concentration measurements and particle-size measurements. The secondary particle size of C_{60} in the DMEM–FBS dispersion was measured by dynamic light scattering (DLS). The diameter of secondary particles was determined using undiluted dispersions and estimated as an average of three measurements obtained using the following devices: DLS spectrophotometer DLS-7000 (632.8 nm; Otsuka Electronics Co., Ltd, Hirakata, Japan), a fibre-optics particle analyser FPAR-1000 (660 nm; Otsuka Electronics Co., Ltd) and a Nanotrac (780 nm; Nikkiso Co., Ltd, Tokyo, Japan). Measurements were performed at a temperature of 25.0 ± 0.1°C. Samples for the particle-size measurement, C_{60} concentration measurement and cytotoxicity assay were obtained from a position 1 cm from the surface of solutions maintained in a static 15-ml tube. Viscosity of the solvent was calculated on the basis of the concentration of free serum albumin in the medium. The C_{60} concentration in the DMEM–FBS dispersion was determined by high-performance liquid chromatography (HPLC). In order to digest adsorbed proteins onto the surface of C_{60}, 30 μl of protease K (Takara Bio Inc., Otsu, Japan) solution at a concentration of 20 mg/ml was added to 2 ml of the C_{60}-DMEM dispersion and incubated for 12 h at 40°C. To extract C_{60}, the dispersion was mixed with 5 ml of toluene, and the solution was agitated for 5 h, sonicated for 15 min and

Table I. Characterization of the fullerene C_{60} in the DMEM–FBS dispersion.

Sample	Code of this study	C_{60} concentration (μg/ml)	Size (nm)		u (nm)	u_{time} (nm)	u_{app} (nm)	u_{method} (nm)	Zeta potential	pH
C_{60}	1	150	d_l	219.3	15.7	0.8	15.5	2.7	−15.8 ± 1.9	8.33
			d_n	124.6	10.4	2.4	4.9	8.8		
	2	68	d_l	211.6	13.0	1.6	12.6	2.7	−14.5 ± 1.5	8.20
			d_n	129.6	12.8	5.7	7.7	8.5		
	3	14	d_l	211.7	16.9	2.5	16.5	3.1	−12.8 ± 1.2	7.61
			d_n	116.9	13.3	0.9	8.5	10.1		
	4	6.6	d_l	213.4	18.5	2.5	18.3	1.8	−12.8 ± 1.3	7.68
			d_n	104.6	17.1	1.8	5.0	16.2		
Control		ND (<0.27)							−10.1 ± 1.8	7.69

d_l: light scattering intensity-averaged diameter; d_n: number-averaged diameter. The value of the C_{60} concentration and zeta potential is the average value 5 days after-preparation. The C_{60} concentration and zeta potential was stable for 5 days after preparation.

centrifuged for 10 min at 2000*g*. The supernatant was filtered using a 0.2 μm-filter unit (Whatman, NJ, USA, PTFE filter) and the precipitate was collected. Next, 5 ml of toluene was added to the precipitate and the same procedure was repeated. The obtained precipitate was washed twice with 1 ml of toluene and filtered using a 0.2-μm filter unit. These extracts were mixed and analysed using HPLC. C_{60} concentrations in the extracts were measured using an HPLC system (Shimadzu Corporation, 10 Avp) equipped with a Develosil column (Nomura Chemical Co. Ltd, Japan) and a UV detector (333 nm). A mixture of toluene–methanol (65:35, v/v) was used as eluent, which was delivered at a rate of 1.0 ml/min.

The zeta potential of the extract was measured at 40 V and 25°C by using a Zetasizer Nano (Malvern Instruments Ltd, Malvern, UK).

Transmission electron microscope observations

Cell specimens exposed to C_{60} were observed using a transmission electron microscope (TEM). The preparation method of TEM specimens was as follows. Cells were fixed using 1.2% glutaraldehyde for 1 h at 4°C and 1% OsO_4 solution for 1 h at 4°C, dehydrated in ethanol, and embedded in epoxy resin. The resulting samples were then cut into ultrathin sections suitable for TEM observations by diamond-knife ultramicrotomy. TEM observations were then carried out using an H-7000 (Hitachi, Japan). The acceleration voltage in the TEM was 75 kV.

Measurement of intracellular oxidative stress

Intracellular ROS were detected using 2′,7′-dichlorofluorescin diacetate (DCFH-DA) (Sigma-Aldrich). A 5 mM stock solution of DCFH-DA was prepared in DMSO, stored at −20°C and diluted 500 times with serum-free medium immediately before use. Cells were exposed to C_{60} dispersion for 2, 6, 12 and 24 h. The dispersion was then changed to fresh serum-free DMEM that included 10 μM of DCFH-DA, and incubated for 30 min at 37°C. Cells were then washed once with PBS, collected by trypsinization, washed once again with PBS and finally resuspended in 500 μl of PBS. The cell samples in PBS were excited with a 488-nm argon ion laser in a Cytomics FC500 flow cytometry system, and the emission of 2′,7′-dichlorofluorescein (DCF) was recorded at 525 nm. Data were collected from at least 5,000 gated events. In addition, the intracellular ROS level of cells exposed to hydrogen peroxide (Wako Pure Chemical Industries, Ltd) at 10–1000 μM was measured as a positive control of the oxidative stress.

Determination of DNA damage

DNA damage by C_{60} was detected by comet assay (*24*) using the CometAssay™ Silver kit (Trevigen, Inc., Gaithersburg, MD, USA) according to the protocol outlined by the manufacturer. The kit included LMAgarose, CometSlide and Lysis Solution. HaCaT cells were exposed to TiO_2–DMEM–FBS dispersion for 24 h, harvested by trypsinization, and resuspended in PBS at 1×10^5 cells/ml. Then the cells were mixed with molten LMAgarose at a ratio of 1 : 10 (v/v), and 75 μl of the mixture was immediately applied onto the CometSlide. Then the slides were immersed in pre-chilled lysis solution and left on ice for 30 min. After removing excessive buffer from the slide, the slide was immersed in alkaline solution (300 mM NaOH, 1 mM EDTA, pH >13) and left for 20 min at room temperature in the dark. Then the slide was washed twice with TBE buffer and electrophoresis was performed using a Mupid submarine electrophoresis system (Advance Co., Ltd, Tokyo, Japan) at 50 V for 2 min. Slides were then rinsed by dipping several times in dH_2O. After the slide was soaked in 70% ethanol for 5 min, electrophoresed DNA was stained by silver staining and counted under the microscope. The level of DNA damage was determined as described by Tayama and Nakagawa (*25*).

Mitochondrial activity and clonogenic assay

For the 3-(4,5-dimethyl-2-thiazolyl)-2,5-diphenyltetrazolium bromide (MTT) assay, cells were seeded in a 96-well plate (Corning) at 1×10^5 cells/well, incubated for 24 h, removed from the culture medium and then exposed to C_{60}-DMEM dispersion or H_2O_2 solution for an additional 6 and 24 h. For the determination of mitochondrial activity, cells were incubated with 0.5 mg/ml MTT (Nacalai Tesque, Inc.) at 37°C for 2 h. Isopropyl alcohol containing 40 mM HCl was added to the culture medium (3:2, by volume) and they were mixed by pipette until the formazan was completely dissolved. The optical density of formazan was measured at 570 nm using a Multiskan Ascent plate reader (Thermo Labsystems, Helsinki, Finland). Cell proliferation was examined by a clonogenic assay based on methods described by Herzog *et al.* (*26*) and Franken *et al.* (*27*). Cells were seeded in six-well microplates (Corning) at a density of 300 cells/well. Each well contained 2 ml of the cell culture medium. Cells were allowed to attach for ∼14 h before they were washed with phosphate buffered saline (PBS) and treated with 2 ml of the centrifuged supernatant. Cells were cultured over the time period required by the control cells to form colonies with a colony being defined as a cluster of at least 50 cells. Here, the time period for culture was set as 7 days. After the culture procedure was completed, the supernatants were removed and the cells were washed once with 2 ml of PBS. Then, the cells were fixed with 100% methanol for 15 min. After the methanol was removed, the cells were stained with Giemsa staining solution (Nacalai Tesque, Inc.), which was diluted 50 times with water, for 15 min and rinsed once with distilled water. Then, the number of colonies was counted. Determination of cell death was detected by the measurement of phosphatidylserine (PS) exposure through the binding of annexin V-FITC, according to the protocol outlined by the manufacturer of the apoptosis detection kit (Medical & Biological Laboratories, Nagoya, Japan). Treated cells were stained with annexin V-FITC and propidium iodide (PI) and analysed with a Cytomics FC500 Flow Cytometry System (Beckman Coulter, Inc., Miami, FL, USA) equipped with a 488-nm argon laser. Data were collected for 10,000 events.

Statistical analysis

Data are expressed as the mean ± S.D. for at least three separate experiments. Statistical analyses were performed by the analysis of variance (ANOVA) using Dunnett or Tukey tests for multiple comparisons. The calculation method has been described in each figure legend.

Results

Characterization of fullerene C_{60} medium dispersion

The results of the characterization of the C_{60}–DMEM dispersion medium are shown in Table I. No precipitate was visible in any of the dispersion mediums. In all C_{60}–DMEM–FBS dispersions, both the light scattering intensity and the average of secondary particle size did not vary throughout the examination period (Fig. 1). Therefore, on the basis of the fact that gravity sedimentation and agglomeration of C_{60} were absent in all the C_{60}–DMEM–FBS dispersions, it can be inferred that the C_{60} secondary particles in the DMEM–FBS dispersion were very stable. In the low concentration C_{60}–DMEM–FBS dispersion medium,

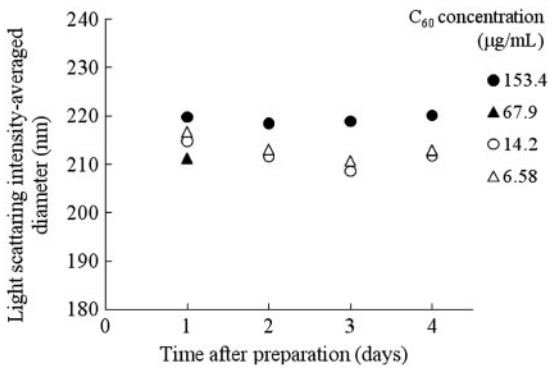

Fig. 1 Stability of size of C_{60} nanoparticles in DMEM–FBS medium dispersion. Light scattering intensities of C_{60} secondary particles were measured by DLS. The C_{60}–DMEM dispersion was prepared at Day 0. Changes to the light scattering intensities during the measurement were small.

the particle size distribution became broad and the number of average sized secondary particles became small by dilution. The pH of the high-concentration C_{60}–DMEM–FBS dispersion was in the basic range.

TEM observation of C_{60} fullerene exposed cells

First, cells that were exposed to C_{60} for 24 h were observed by TEM (Fig. 2). The C_{60} was taken up into the cell as aggregates in both HaCaT and A549 cells. Internalized C_{60} aggregates were distributed in the cytoplasm within phagosome-like structures. Re-dispersion and nuclear entry of C_{60} was not observed. Internalized C_{60} aggregates were larger than the particle measured by DLS, suggesting that the aggregates accumulated in the cytoplasm. Internalized C_{60} aggregates did fuse to lysosomes as previously observed in platinum exposed cells (*28*, *29*). Some aggregates formed lamellar cup-shaped lysosomes in the cytoplasm in A549 cells (Fig. 2E and F).

Interestingly, the particle size of the internalized C_{60} aggregates and the number-averaged diameter (d_n) of the C_{60} aggregates in the DMEM–FBS dispersion measured by DLS differed. In DMEM–FBS, C_{60} formed aggregates of 100–130 nm, while the particle size of internalized C_{60} aggregates were larger at ~1.7–2.0 μm, as determined by TEM. There are two hypotheses for this observation, either agglomeration of the aggregates in the cells, or selective uptake of aggregates of particular size. However, the C_{60}–DMEM–FBS dispersion used in this study was very stable and uniform during the examination period, suggesting that the intracellular agglomeration hypothesis is more likely.

Oxidative stress to cultured cells induced by fullerene C_{60}

There are reports that some nanoparticles may induce oxidative stress in culture cells (*30*, *31*). Since uptake of the C_{60} secondary particles was observed (Fig. 2), intracellular oxidative stress levels were examined. Intracellular oxidative stress induced by C_{60} exposure was measured using the DCFH method (Fig. 3A). Intracellular ROS levels in C_{60} exposed HaCaT cells increased over time. Intracellular ROS levels increased ~2- to 3-fold compared with control cells in both HaCaT and A549 cells that were exposed to high concentrations of C_{60} for 24 h. In contrast, the intracellular ROS levels in cells that were exposed to the low concentrations of C_{60} did not increase. Also, the influence of fullerene C_{60} on intracellular ROS levels was compared with H_2O_2, which was used as a positive control for oxidative stress (Fig. 3B). The increase in the intracellular ROS level induced by 153.4 μg/ml of fullerene C_{60} was comparable with exposure to 100–250 μM H_2O_2. In comparison with the cells exposed to C_{60}, the rate of increase in intracellular ROS levels over time was larger in the H_2O_2 exposed cells. The intracellular ROS level could not be measured in HaCaT cells which were exposed to 1,000 μM H_2O_2 for 24 h, because almost all the cells were killed.

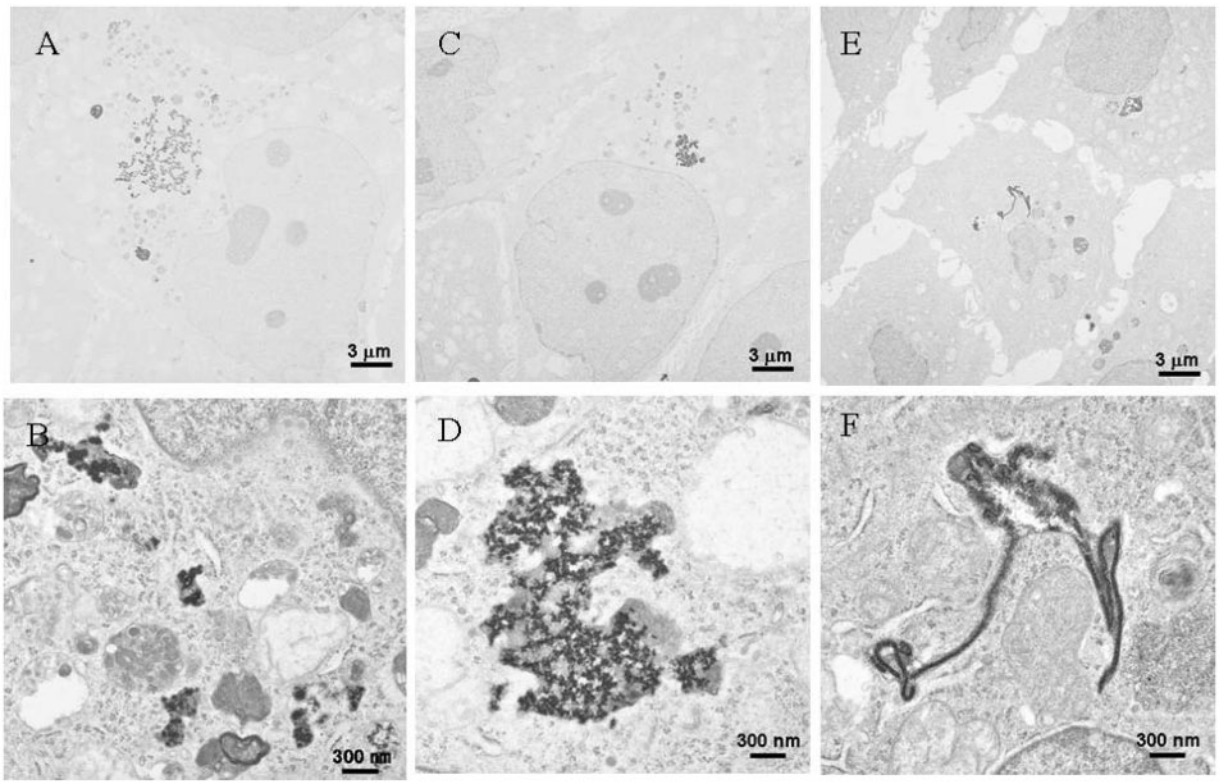

Fig. 2 Transmission electron microscope observations of cells exposed to C_{60}. (A–D) HaCaT cells exposed to the C_{60}–DMEM–FBS dispersion for 24 h. (E and F) A549 cells exposed to the C_{60}–DMEM–FBS dispersion for 24 h.

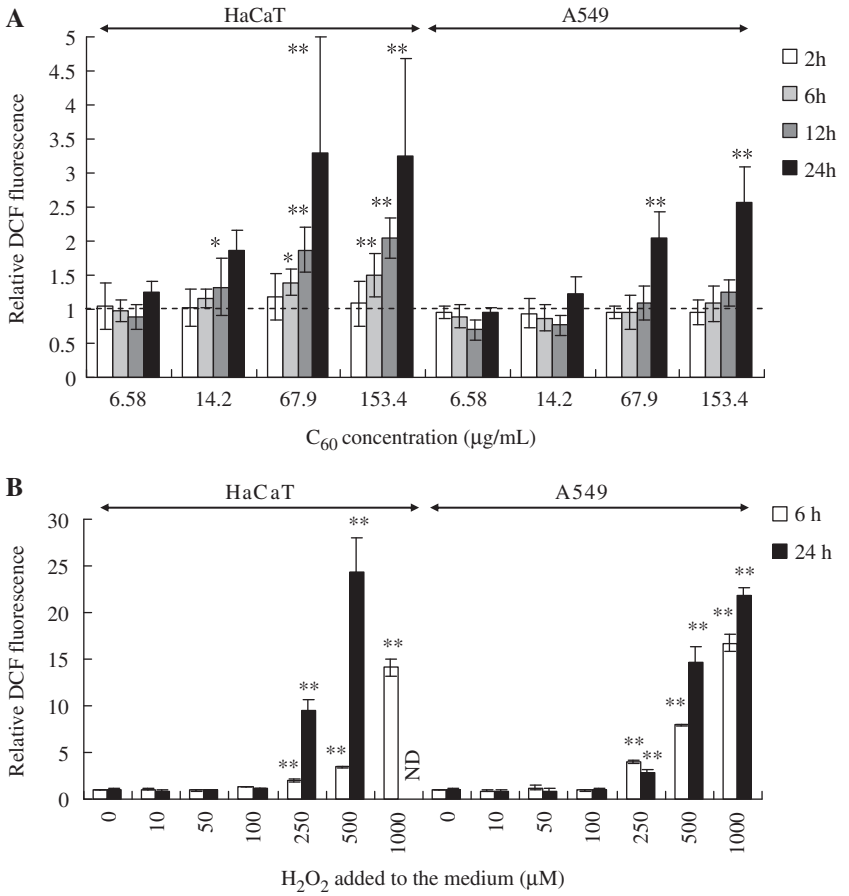

Fig. 3 Intracellular oxidative stress level in cells exposed to the C_{60}–DMEM–FBS dispersion and H_2O_2. (A) Intracellular ROS levels in cells exposed to the C_{60}–DMEM–FBS dispersion. The cells were exposed to the C_{60}–DMEM–FBS dispersion for 2, 6, 12 and 24 h. (B) Intracellular ROS level in cells exposed to H_2O_2. The cells were exposed to the medium including H_2O_2 for 6 and 24 h. The medium was exchanged with fresh, FBS-free DMEM containing 10 μM DCFH-DA. After incubation for 30 min, cells were collected and washed. DCFH fluorescence in the cell was then measured by flow cytometry. The value of the DCFH fluorescence standardized control was 1. Values are the averages and S.D. of three independent experiments. $*P<0.05$; $**P<0.01$ (Dunnett, ANOVA).

Influence of fullerene C_{60} on MTT conversion and colony formation

Since mild oxidative stress is said to induce apoptosis (*32*), mitochondrial enzyme activity was measured as an index of living cells. The fullerene C_{60}-DMEM dispersion was applied to HaCaT and A549 cells and mitochondrial activity was measured after 6 and 24 h using the MTT assay (Fig. 4A). Neither HaCaT nor A549 cells showed a decrease in MTT conversion. In addition, cellular effects of fullerene C_{60} were compared with H_2O_2 (Fig. 4B). Although C_{60} exposure did not induce reduction in MTT conversion, H_2O_2 exposure induced cell death. These results suggest that the cellular effect of C_{60} is milder than H_2O_2, but they produce similar levels of oxidative stress (Fig. 3).

Cell viability was also measured by flow cytometry (Fig. 4C and D). Cells exposed to C_{60}-DMEM dispersion and H_2O_2 for 24 h were stained with annexin V-FITC, and PI and fluorescence was measured by flow cytometry. H_2O_2 induced apoptosis of HaCaT and A549 cells at 250 μM. This result conforms to the H_2O_2 findings in which intracellular ROS levels and reduction of cell viability were induced. In contrast, compared to the control cells, both the annexin V-FITC and PI fluorescence did not increase significantly in C_{60} exposed cells (Fig. 4C), indicating that C_{60} did not induce apoptosis or necrosis in cultured cells following 24 h of exposure. On the other hand, C_{60} inhibited cell proliferation (Fig. 5A). In particular, growth inhibition was observed in cells that were exposed to high concentrations of C_{60}: The colonies of HaCaT cells cultured without C_{60} and with low concentrations of C_{60} were composed of 50 cells or more. In contrast, colonies of cells cultured with high concentrations of C_{60} were composed of 10 cells or less; and when A549 cells were exposed to high concentrations of C_{60}, the colonies were composed of 30 cells or less (Fig. 5B).

DNA damage induced by fullerene C_{60}

In many cases, increases in intracellular oxidative stress levels induce DNA damage (*33*, *34*). C_{60} fullerene has been reported to be associated with oxidative damage to DNA (*35*). Therefore, induction of DNA damage following C_{60} exposure was examined by comet assay (Fig. 6). A concentration-dependent increase in DNA damage was observed following

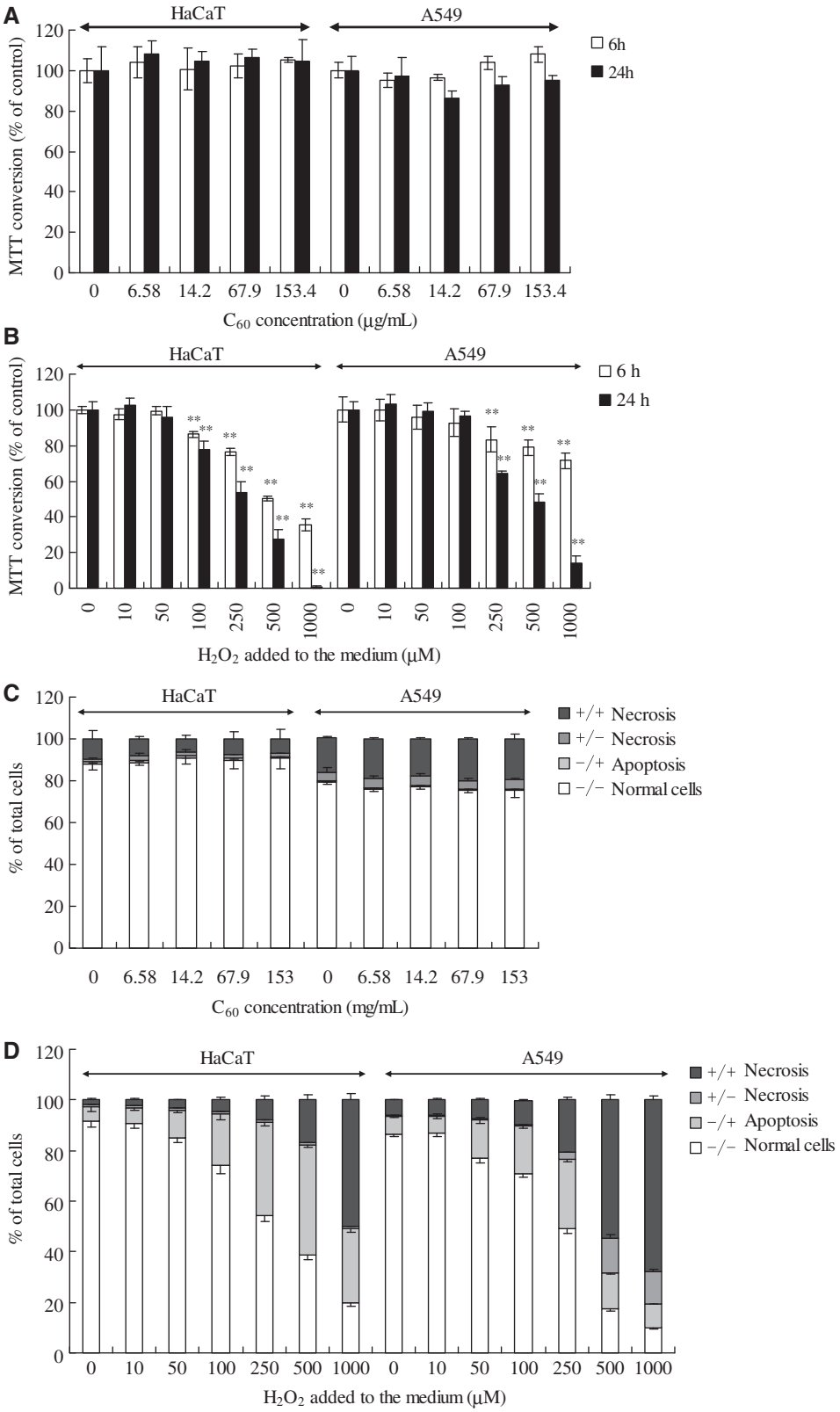

Fig. 4 Influence of C_{60}–DMEM–FBS dispersion on cell viability. (A and B) Comparison of the effects of fullerene C_{60} and H_2O_2 on cells. (A) Effect of C_{60}–DMEM–FBS dispersion on mitochondrial enzyme activity. The HaCaT and A549 cells were exposed to the C_{60}–DMEM–FBS dispersion. Secondary particle sizes of C_{60} in dispersions were measured by DLS simultaneously with the MTT assay. (B) Effect of H_2O_2 on intracellular ROS level and mitochondrial enzyme activity. The cells were treated with the dispersion for 6 (opened column) and 24 h (closed column), and the mitochondrial enzyme activity was measured by the MTT assay. The percentage of mitochondrial enzyme activity compared with the standardized control was 100%. Intracellular ROS level was measured by the same procedure described in Fig. 3. (C and D) Detection of apoptotic cells following C_{60} and H_2O_2 exposure. The cells were exposed to the C_{60}–DMEM–FBS dispersion and H_2O_2 for 24 h. Subsequently, the cell samples were treated with PI and annexin V-FITC and analysed by flow cytometry. The data indicates the rate of PI/annexin V positive (+) or negative (–) cells. The data are presented as the percentage of each cell from 10,000 cells. Values are averages of three independent experiments. $^{**}P<0.01$ (vs control, Dunnett, ANOVA).

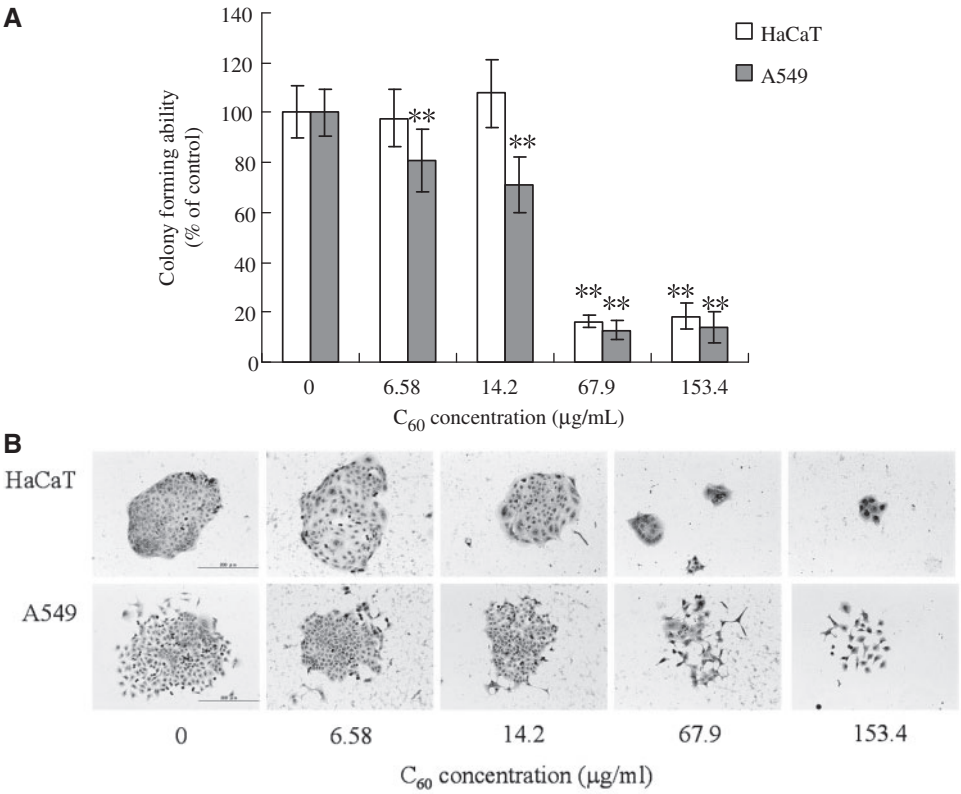

Fig. 5 Effect of C_{60}–DMEM–FBS dispersion on cell proliferation. HaCaT and A549 cells were exposed to C_{60}–DMEM–FBS dispersion. The cell proliferation was measured by the clonogenic assay. The cells were then cultured with the C_{60}–DMEM–FBS dispersion for 7 days before the number of colonies was counted. (A) Cell proliferation standardized to control (100%). $^{**}P < 0.01$ (vs control, Dunnett, ANOVA). (B) Typical colony cultured in C_{60} dispersion at each concentration. The bar indicates 200 μm.

C_{60} exposure. High concentrations of C_{60} remarkably induced DNA damage in both HaCaT and A549 cells.

Discussion

In this study, cellular responses induced by pristine fullerene C_{60} were examined using stable dispersion. A uniform and stable C_{60}-medium dispersion without chemical dispersant was successfully prepared. To investigate the cellular responses induced by C_{60}, high concentrations (150 and 68 μg/ml) and low concentrations (14 and 6.6 μg/ml) of C_{60}–DMEM–FBS dispersions were applied to cultured cells. Exposure to high concentrations of C_{60} led to an increase in intracellular ROS levels (Fig. 3A). This effect is likely due to the intracellular influence of C_{60} since intracellular ROS levels increased over time in the C_{60} exposed cells.

Although fullerene C_{60} has photocytotoxicity via induction of oxidative stress (*36*), C_{60} was not irradiated by light in the present study indicating that pristine C_{60} potentially has the ability to induce cellular oxidative stress without photoactivation. The oxidative stress induced by C_{60} did not affect cell viability after 24 h of exposure (Fig. 4). The cellular responses induced by fullerene C_{60} were different from responses induced by H_2O_2, the oxidative stress positive control, which induced oxidative stress and subsequently cell death. In H_2O_2-induced cell death, the induction of apoptosis and necrosis occurred in a concentration dependent manner (*37*). Even though intracellular ROS were induced to similar levels, C_{60} treatment did not lead to a decrease in cell viability while H_2O_2 led to cell death. Also, C_{60} did not induce apoptosis or necrosis. This result suggests that the mechanism behind the cellular effects induced by C_{60} and H_2O_2 is different. Meanwhile, C_{60} inhibited cell proliferation. In the clonogenic assay, cells that were exposed to high concentrations of C_{60} had a smaller number of colonies that were composed of fewer cells, particularly for HaCaT cells (Fig. 5). These results indicate that C_{60} influences cell growth without affecting cell viability.

The influence of C_{60} exposure on nucleic acids was also remarkable, with a concentration dependent effect of C_{60} on DNA damage. It has been reported that light exposed fullerenes produce singlet oxygen (*38*, *39*) and that singlet oxygen produced by C_{60} can induce DNA damage in *Salmonella typhimurium* (*6*). In this study, DNA damage by C_{60} was observed in mammalian cells. TEM observations showed cellular uptake of C_{60} aggregates distributed in the cytoplasm but they did not enter the nucleus (Fig. 2). Considering that DNA is generally protected by the nuclear membrane in eukaryotic cells, our findings suggest that C_{60} did not directly attack the nucleic acid in the nucleus. However, the mechanism of DNA damage induced by C_{60} is still not fully understood and it is difficult to explain why induction of oxidative stress and DNA injury did not lead to cell death. Many nano-objects such as TiO_2 and CNT frequently induce cell death with via oxidative stress and DNA injury (*40*, *41*).

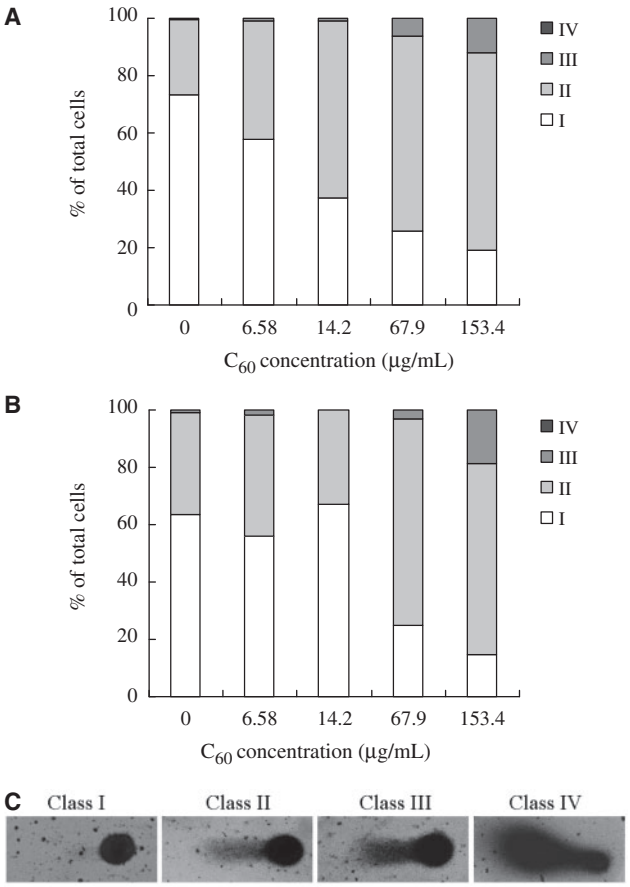

Fig. 6 DNA damage in cells exposed to the C_{60}–DMEM–FBS dispersion. HaCaT (A) and A549 (B) cells were exposed to the C_{60}–DMEM–FBS dispersion for 24 h and DNA damage measured by the comet assay. Approximately 200 cells were counted and the DNA damage was classified according to the classifications described by Tayama and Nakagawa (*25*). (C) A typical image of each class is shown under the graph.

However, induction of oxidative stress and DNA injury by fullerene C_{60} did not lead to cell death but instead seemed to influence cell proliferation. The interaction of mechanisms of cell death and oxidative stress induced by fullerene C_{60} is currently under further investigation.

These results suggest that the major influence of C_{60} on the cultured cells is induction of oxidative stress caused by the uptake of aggregates, thereby inhibiting growth. When C_{60} was applied to cells, cellular uptake of C_{60} secondary particles occurred then internalized C_{60} particles induced mild oxidative stress to the cells. The oxidative stress induced by C_{60} could be reduced by the cellular anti-oxidative defence system, such as through the haem oxygenase-1 system. Therefore, C_{60} did not induce remarkable levels of cell death. However, *in vivo*, these results suggest the possibility that intracellular C_{60} may persist for a long time without clearance by macrophages. In particular, the metabolic stability of C_{60} in the lung may lead to severe diseases and may be compared to the toxicity of asbestos (*42–45*). Inhaled asbestos stays in the lung for long periods of time by escaping from the immune system and consecutively induces DNA injury through iron-derived ROS. In some cases, poorly soluble particles have genotoxic potential by direct and indirect generation of ROS (*46*, *47*). Asbestos and other toxic particles, such as crystalline silica and diesel exhaust particles (DEP), induced DNA strand breaks in cells (*48–50*).

Although it is uncertain whether DNA damage by C_{60} is a direct or indirect effect, C_{60}-derived DNA injury is of great importance for risk assessment of C_{60}. Many mild but prolonged periods of cellular oxidative stress could be induced by C_{60} leading to secondary effects, such as lipid peroxidation and DNA injury. *In vivo*, inhalation of C_{60} may induce prolonged oxidative stress in the lung and subsequently lead to fibrosis or tumour formation. The results obtained from long term exposure *in vivo* experiments are essential for an accurate risk assessment of C_{60}, including the data of clearance of C_{60} in the lung. It has been reported that the lung half-life for C_{60} is approximately one month (*51*). The influence of C_{60} will be smaller *in vivo*, because C_{60} can be cleared by the alveolar macrophages and a more complex antioxidant defence system exists (*52*). Overall, the results obtained from this study indicate that C_{60} has a toxic potential. In contrast to other modified C_{60} forms, which have anti-oxidative activity (*11*, *53*), pristine C_{60} induces oxidative stress. Because the metabolism of these modified C_{60} forms in the body is unclear, the assessment of the biological activity of C_{60} and its derivatives is ongoing.

Acknowledgements

The authors would like to thank Ms Emiko Kobayashi (National Institute of Advanced Industrial Science and Technology, Japan) for help in performing the TEM observations.

Funding

This work was funded by a New Energy and Industrial Technology Development Organization (NEDO) Grant 'Evaluating risks associated with manufactured nanomaterials (P06041)'.

Conflict of interest

None declared.

References

1. Kroto, H.W., Heath, J.R., O'Brien, S.C., Curl, R.F., and Smalley, R.E. (1985) C_{60}: Buckminsterfullerene. *Nature* **318**, 162–163
2. Bosi, S., Da Ros, T., Spalluto, G., and Prato, M. (2003) Fullerene derivatives: an attractive tool for biological applications. *Eur. J. Med. Chem.* **38**, 913–923
3. Cai, X., Jia, H., Liu, Z., Hou, B., Luo, C., Feng, Z., Li, W., and Liu, J. (2008) Polyhydroxylated fullerene derivative C(60)(OH)(24) prevents mitochondrial dysfunction and oxidative damage in an MPP(+)-induced cellular model of Parkinson's disease. *J. Neurosci. Res.* **86**, 3622–3634
4. Bogdanović, V., Stankov, K., Icević, I., Zikic, D., Nikolić, A., Solajić, S., Djordjević, A., and Bogdanović, G. (2008) Fullerenol $C_{60}(OH)_{24}$ effects on antioxidative enzymes activity in irradiated hum an erythroleukemia cell line. *J. Radiat. Res.* **49**, 321–327

5. Hu, Z., Guan, W., Wang, W., Huang, L., Xing, H., and Zhu, Z. (2007) Protective effect of a novel cystine C(60) derivative on hydrogen peroxide-induced apoptosis in rat pheochromocytoma PC12 cells. *Chem. Biol. Interact.* **167**, 135–144
6. Sera, N., Tokiwa, H., and Miyata, N. (1996) Mutagenicity of the fullerene C_{60}-generated singlet oxygen dependent formation of lipid peroxides. *Carcinogenesis* **17**, 2163–2169
7. Sayes, C.M., Gobin, A.M., Ausman, K.D., Mendez, J., West, J.L., and Colvin, V.L. (2005) Nano-C_{60} cytotoxicity is due to lipid peroxidation. *Biomaterials* **26**, 7587–7595
8. Sayes, C.M., Marchione, A.A., Reed, K.L., and Warheit, D.B. (2007) Comparative pulmonary toxicity assessments of C60 water suspensions in rats: few differences in fullerene toxicity in vivo in contrast to in vitro profiles. *Nano Lett* **8**, 2399–2406
9. Isakovic, A., Markovic, Z., Todorovic-Markovic, B., Nikolic, N., Vranjes-Djuric, S., Mirkovic, M., Dramicanin, M., Harhaji, L., Raicevic, N., Nikolic, Z., and Trajkovic, V. (2006) Distinct cytotoxic mechanisms of pristine versus hydroxylated fullerene. *Toxicol. Sci.* **91**, 173–183
10. Sayes, C.M., Fortner, J.D., Guo, W., Lyon, D., Boyd, A.M., Ausman, K.D., Tao, Y.J., Sitharaman, B., Wilson, L.J., Hughes, J.B., West, J.L., and Colvin, V.L. (2004) The differential cytotoxicity of water-soluble fullerenes. *Nano Lett* **4**, 1881–1887
11. Takada, H., Kokubo, K., Matsubayashi, K., and Oshima, T. (2006) Antioxidant activity of supramolecular water-soluble fullerenes evaluated by beta-carotene bleaching assay. *Biosci. Biotechnol. Biochem.* **70**, 3088–93
12. Park, E.J., Kim, H., Kim, Y., Yi, J., Choi, K., and Park, K. (2010) Carbon fullerenes (C60s) can induce inflammatory responses in the lung of mice. *Toxicol. Appl. Pharmacol.* **244**, 226–233
13. Chen, K.L. and Elimelech, M. (2006) Aggregation and deposition kinetics of fullerene (C_{60}) Nanoparticles. *Langmuir* **22**, 10994–11001
14. Heath, J.R., O'Brien, S.C., Zhang, Q., Liu, Y., Curl, R.F., Tittel, F.K., and Smalley, R.E. (1985) Lanthanum complexes of spheroidal carbon shells. *J. Am. Chem. Soc.* **107**, 7779–7780
15. Teeguarden, J.G., Hinderliter, P.M., Orr, G., Thrall, B.D., and Pounds, J.G. (2007) Particokinetics in vitro: dosimetry considerations for in vitro nanoparticle toxicity assessments. *Toxicol. Sci.* **95**, 300–312
16. Limbach, L.K., Li, Y., Grass, R.N., Brunner, T.J., Hintermann, M.A., Muller, M., Gunther, D., and Stark, W.J. (2005) Oxide nanoparticle uptake in human lung fibroblasts: effects of particle size, agglomeration, and diffusion at low concentrations. *Environ. Sci. Technol.* **39**, 9370–9376
17. Jensen, A.W., Wilson, S.R., and Schuster, D.I. (1996) Biological applications of fullerenes. *Bioorg. Med. Chem.* **4**, 767–779
18. Tsuchiya, T., Oguri, I., Yamakoshi, Y.N., and Miyata, N. (1996) Novel harmful effects of [60]fullerene on mouse embryos *in vitro* and *in vivo*. *FEBS Lett* **393**, 139–145
19. Han, B. and Karim, M.N. (2008) Cytotoxicity of aggregated fullerene C_{60} particles on CHO and MDCK cells. *Scanning* **30**, 213–220
20. Takagi, A., Hirose, A., Nishimura, T., Fukumori, N., Ogata, A., Ohashi, N., Kitajima, S., and Kanno, J. (2008) Induction of mesothelioma in p53+/- mouse by intraperitoneal application of multi-wall carbon nanotube. *J. Toxicol. Sci.* **33**, 105–116
21. Tatsuishi, T., Oyama, Y., Iwase, K., Yamaguchi, J.Y., Kobayashi, M., Nishimura, Y., Kanada, A., Hampton, M.B., Fadeel, B., and Orrenius, S. (1998) Redox regulation of the caspases during apoptosis. *Ann. NY Acad. Sci.* **854**, 328–335
22. Deguchi, S., Yamazaki, T., Mukai, S.A., Usami, R., and Horikoshi, K. (2007) Stabilization of C_{60} nanoparticles by protein adsorption and its implications for toxicity studies. *Chem. Res. Toxicol.* **20**, 854–858
23. Buford, M.C., Hamilton, R.F. Jr, and Holian, A.A. (2007) comparison of dispersing media for various engineered carbon nanoparticles. *Part Fibre Toxicol.* **4**, 6
24. Singh, N.P., McCoy, M.T., Tice, R.R., and Schneider, E. L. (1988) A simple technique for quantitation of low levels of DNA damage in individual cells. *Exp. Cell Res.* **175**, 184–191
25. Tayama, S. and Nakagawa, Y. (2004) Comet assay attempted with silver staining method and manual microscopic analysis using CHO-K1 cells. *Ann. Rep. Tokyo Metr. Inst. P.H.* **55**, 315–318
26. Herzog, E., Casey, A., Lyng, F.M., Chambers, G., Byrne, H.J., and Davoren, M. (2007) A new approach to the toxicity testing of carbon-based nanomaterials – the clonogenic assay. *Toxicol. Lett.* **174**, 49–60
27. Franken, N.A., Rodermond, H.M., Stap, J., Haveman, J., and van Bree, C. (2006) Clonogenic assay of cells *in vitro*. *Nat. Protoc.* **1**, 2315–9
28. Ghadially, F.N., Lock, C.J., Lalonde, J.M., and Ghadially, R. (1981) Platinosomes produced in synovial membrane by platinum coordination complexes. *Virchows. Arch. B Cell. Pathol. Incl. Mol. Pathol.* **35**, 123–131
29. Ghadially, F.N., Lock, C.J., Yang-Steppuhn, S.E., and Lalonde, J.M. (1981) Platinosomes produced in cultured cells by platinum coordination complexes. *J. Submicrosc. Cytol.* **13**, 223–230
30. Bhattacharya, K., Davoren, M., Boertz, J., Schins, R.P., Hoffmann, E., and Dopp, E. (2009) Titanium dioxide nanoparticles induce oxidative stress and DNA-adduct formation but not DNA-breakage in human lung cells. *Part. Fibre. Toxicol.* **21**, 17
31. Eom, H.J. and Choi, J. (2009) Oxidative stress of silica nanoparticles in human bronchial epithelial cell, Beas-2B. *Toxicol. In Vitro*. **23**, 1326–1332
32. Hampton, M.B. and Orrenius, S. (1998) Redox regulation of apoptotic cell death. *Biofactors* **8**, 1–5
33. Inoue, S. and Kawanishi, S. (1995) Oxidative DNA damage induced by simultaneous generation of nitric oxide and superoxide. *FEBS Lett* **371**, 86–88
34. Franco, R., Schoneveld, O., Georgakilas, A.G., and Panayiotidis, M.I. (2008) Oxidative stress, DNA methylation and carcinogenesis. *Cancer Lett* **266**, 6–11
35. Folkmann, J.K., Risom, L., Jacobsen, N.R., Wallin, H., Loft, S., and Møller, P. (2009) Oxidatively damaged DNA in rats exposed by oral gavage to C_{60} fullerenes and single-walled carbon nanotubes. *Environ. Health Perspect.* **117**, 703–708
36. Zhao, B., He, Y.Y., Bilski, P.J., and Chignell, C.F. (2008) Pristine (C60) and hydroxylated [C60(OH)24] fullerene phototoxicity towards HaCaT keratinocytes: type I vs type II mechanisms. *Chem. Res. Toxicol.* **21**, 1056–1063
37. Saito, Y., Nishio, K., Ogawa, Y., Kimata, J., Kinumi, T., Yoshida, Y., Noguchi, N., and Niki, E. (2006) Turning point in apoptosis/necrosis induced by hydrogen peroxide. *Free Radic. Res.* **40**, 619–630
38. Yamakoshi, Y., Umezawa, N., Ryu, A., Arakane, K., Miyata, N., Goda, Y., Masumizu, T., and Nagano, T. (2003) Active oxygen species generated from

photoexcited fullerene (C_{60}) as potential medicines: O_2-* versus $^1O_2$. *J. Am. Chem. Soc.* **125**, 12803–12809
39. Arbogast, J.W. and Foote, C.S. (1991) Photophysical properties of C70. *J. Am. Chem. Soc.* **113**, 8886–8889
40. Reeves, J.F., Davies, S.J., Dodd, N.J., and Jha, A.N. (2008) Hydroxyl radicals (*OH) are associated with titanium dioxide (TiO(2)) nanoparticle-induced cytotoxicity and oxidative DNA damage in fish cells. *Mutat. Res.* **640**, 113–122
41. Patlolla, A., Patlolla, B., and Tchounwou, P. (2010) Evaluation of cell viability, DNA damage, and cell death in normal human dermal fibroblast cells induced by functionalized multiwalled carbon nanotube. *Mol. Cell Biochem.* **338**, 225–232
42. Arul, K.J. and Holt, P.F. (1980) Clearance of asbestos bodies from the lung: a personal view. *Br J. Ind. Med.* **37**, 273–277
43. Finkelstein, M.M. and Dufresne, A. (1999) Inferences on the kinetics of asbestos deposition and clearance among chrysotile miners and millers. *Am J. Ind. Med.* **35**, 401–412
44. Kamp, D.W. (2009) Asbestos-induced lung diseases: an update. *Transl. Res.* **153**, 143–152
45. Vallyathan, V., Shi, X., and Castranova, V. (1998) Reactive oxygen species: their relation to pneumoconiosis and carcinogenesis. *Environ. Health Perspect.* **106**, 1151–1155
46. Knaapen, A.M., Borm, P.J., Albrecht, C., and Schins, R.P. (2004) Inhaled particles and lung cancer. Part A: Mechanisms. *Int. J. Cancer* **109**, 799–809
47. Schins, R.P. and Knaapen, A.M. (2007) Genotoxicity of poorly soluble particles. *Inhal. Toxicol.* **19**, 189–198
48. Levresse, V., Renier, A., Levy, F., Broaddus, V.C., and Jaurand, M. (2000) DNA breakage in asbestos-treated normal and transformed (TSV40) rat pleural mesothelial cells. *Mutagenesis* **15**, 239–244
49. Zhong, B.Z., Whong, W.Z., and Ong, T.M. (1997) Detection of mineral-dust-induced DNA damage in two mammalian cell lines using the alkaline single cell gel/comet assay. *Mutat. Res.* **393**, 181–187
50. Don Porto Carero, A., Hoet, P.H., Verschaeve, L., Schoeters, G., and Nemery, B. (2001) Genotoxic effects of carbon black particles, diesel exhaust particles, and urban air particulates and their extracts on a human alveolar epithelial cell line (A549) and a human monocytic cell line (THP-1). *Environ. Mol. Mutagen.* **37**, 155–163
51. Baker, G.L., Gupta, A., Clark, M.L., Valenzuela, B.R., Staska, L. M., Harbo, S. J., Pierce, J. T., and Dill, J. A. (2008) Inhalation toxicity and lung toxicokinetics of C60 fullerene nanoparticles and microparticles. *Toxicol. Sci.* **101**, 122–131
52. Matalon, S., Holm, B.A., Baker, R.R., Whitfield, M.K., and Freeman, B.A. (1990) Characterization of antioxidant activities of pulmonary surfactant mixtures. *Biochim. Biophys. Acta.* **1035**, 121–127
53. Lin, A.M., Chyi, B.Y., Wang, S.D., Yu, H.H., Kanakamma, P.P., Luh, T.Y., Chou, C.K., and Ho, L.T. (1999) Carboxyfullerene prevents iron-induced oxidative stress in rat brain. *J. Neurochem.* **72**, 1634–1640